

Polarization-independent optical racetrack resonators using rib waveguides on silicon-on-insulator

William R. Headley,^{a)} Graham T. Reed, and Simon Howe

Advanced Technology Institute, University of Surrey, Daphne Jackson Building, Guildford, Surrey GU2 7XH, United Kingdom

Ansheng Liu and Mario Paniccia

Intel Corporation, 2200 Mission College Boulevard, CHP3-109, Santa Clara, California 95054

(Received 22 April 2004; accepted 24 September 2004)

In an effort to find low-cost alternatives for components currently used in dense wavelength division multiplexing, optical ring resonators fabricated on silicon on insulator are currently being investigated. Their performance can be further enhanced if they are polarization independent. Herein we use rib waveguides to control the polarization properties of the devices and hence produce polarization-independent racetrack ring resonators. Transverse electric and transverse magnetic resonant peaks are measured to within 2 pm of one another over four cycles of the free spectral range. The racetrack resonators also exhibit measured Q factors of approximately 90 000 and finesse values of 12. © 2004 American Institute of Physics. [DOI: 10.1063/1.1827337]

An optical ring resonator is a versatile device that can then be utilized to create many different optical devices, including filters,^{1,2} switches,^{3,4} and add-drop multiplexers⁵ for use in dense wavelength division multiplexing systems. In high index media such as silicon on insulator, (SOI), most ring resonator devices realized thus far are made using strip, or photonic wire waveguides.^{6,7} This is to allow for the small bend radii necessary to minimize the loss associated with devices and hence to produce a large free spectral range (FSR). However, the use of strip waveguides makes it much more difficult to control the polarization properties of the resultant devices. In this work we take an alternative approach, designing optical racetrack resonators based upon rib waveguides, to allow us to optimize control of the polarization properties and therefore realize a polarization-independent ring resonator. While a polarization-independent ring resonator has been demonstrated in the low index contrast material of silicon oxynitride, our devices are fabricated in single-crystal SOI. The design and fabrication is discussed first, followed by presentation and discussion of experimental results.

In order to design a polarization-independent ring resonator, the first step was to investigate the polarization characteristics of the rib waveguide due to its geometry. The BEAMPROP⁸ simulation package was used to determine the dimensions necessary to create such a device. The initial height and width were set to 1.35 and 1 μm , respectively. These dimensions were chosen in order to maintain as large a device as possible (within the constraints of the rib height) for ease of coupling light to the device. Using BEAMPROP, the effective indices of the fundamental TE and TM waveguide modes were monitored as the etch depth was varied. Figure 1(a) shows a plot of the effective index as a function of etch depth for both polarizations. The etch depth at which the two curves cross indicates that both TE and TM polarizations have the same effective index and therefore the waveguide is polarization independent in terms of propagation constant.

Next it was necessary to design a polarization-independent directional coupler. Figure 1(b) shows a typical result of modeling a directional coupler using BEAMPROP. For the purposes of the modeling, the left arm of the coupler was excited with an optical field. Figure 1(b) shows that with propagation distance z , light transfers from the left waveguide to the right, and back again in a cyclic manner. The

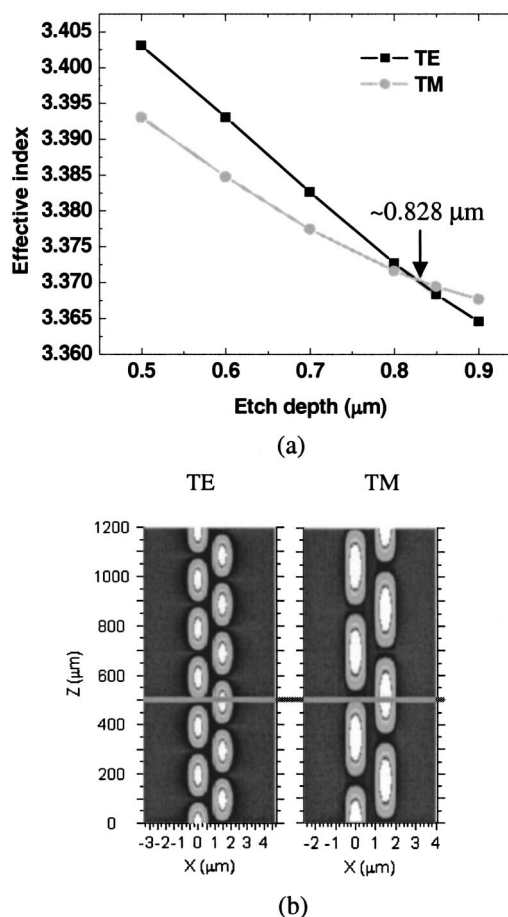
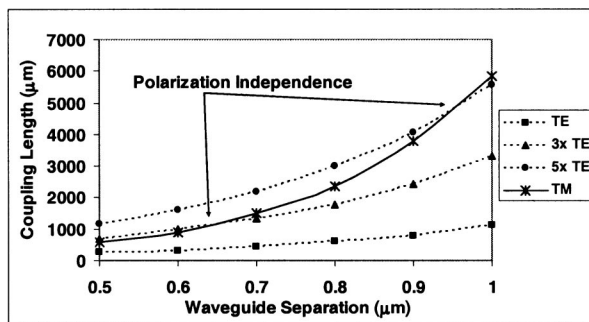
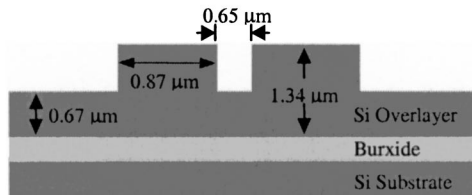


FIG. 1. (a) Determination of a polarization independent rib waveguide and (b) directional coupler.

^{a)}Electronic mail: w.headley@surrey.ac.uk



(a)



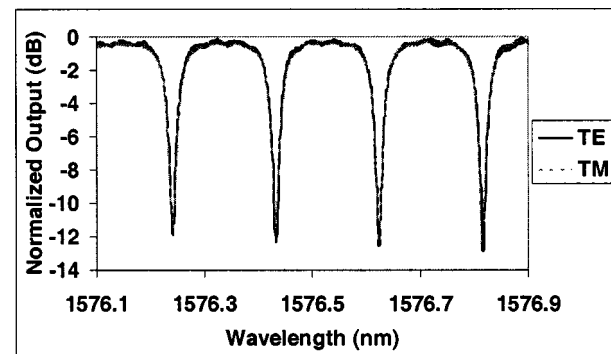
(b)

FIG. 2. (a) Determination of a polarization independent directional coupler and (b) the dimensions of the coupler taken from a SEM image of an actual device.

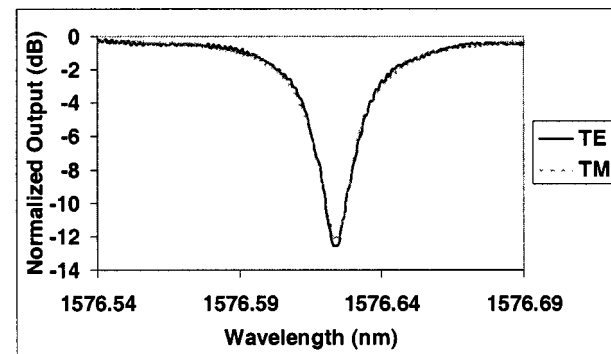
goal of the modeling is to find a coupler length that yields total power transfer from the left waveguide to the right, for both polarizations. This, in effect, means that all of the power is transferred from the input waveguide to the ring waveguide for whichever polarization is excited. Figure 2(a) shows the results of varying the separation of the waveguides that form the coupler, as a function of the coupling length. Several curves are plotted, for each polarization. The dimensions of the ribs used to model the coupler were determined from the results of Fig. 1(a). If a point can be found where the two different polarization curves intersect, this gives the coupling length and waveguide separation necessary to define a polarization-independent directional coupler.

Figure 2(a) demonstrates that, for the above-mentioned coupler dimensions, the TE and TM curves do not intersect. However, as can be seen from Fig. 1(b), power transfers in a shorter length for the TE polarization than for TM. Hence, in Fig. 2(a), curves are also plotted for TE polarized light, where the power makes three (labeled 3 \times) and five (labeled 5 \times) complete transitions between the two waveguides. These two curves do intersect with the TM curve and therefore define a coupler length and waveguide separation where total power transfer occurs for both polarization modes. Thus a polarization-independent coupler can be designed.

Polarization-independent waveguides and couplers form the building blocks of a polarization-independent ring resonator. However, because of tolerances associated with device processing, a matrix of resonators was fabricated with a variety of dimensions based around the above-modeled dimensions. Several wafers with slightly differing etch depths were also processed for the same reason. Figure 2(b) shows the dimensions of one alternative design, which departs slightly from the above-established dimensions. For example, the rib height is now 1.34 μm rather than 1.35 μm . Similarly the etch depth is 0.67 μm rather than 0.828 μm defined in Fig.



(a)



(b)

FIG. 3. (a) Spectral response of the fabricated racetrack resonator and the (b) close-up of the peak at 1576.624 nm.

1(a). This device was subsequently modeled and the results are shown in Fig. 1(b). The gray line shows that all of the power has transferred from the left arm to the right for both polarizations. Thus for a coupling length of 500 μm at 1550 nm, this directional coupler is polarization independent. Hence there are clearly a range of designs that retain polarization-independent operation, while the matrix design approach allows for processing variations. Because of the relatively long couplers used, the ring now has a racetrack appearance.

Due to the use of polarization-independent rib waveguides the ring resonator design incorporated a bend radius of 400 μm to minimize the bend loss of these rib waveguides, and was fabricated in SIMOX material from the IBIS Corporation.⁹ The initial thickness of the silicon overlayer was 1.5 μm with a buried oxide thickness of 0.375 μm . A hard mask was grown on the wafer to facilitate the etch process. The hard mask consumed approximately 150 nm of the initial overlayer thickness so that the final waveguide heights are nominally 1.35 μm . After etching, the devices were covered with a passivating surface oxide. This was carried out to provide some protection to the waveguides during end facet preparation.

The wafers were then diced and the end facets polished. The end facets of each die were antireflection coated in order to minimize Fresnel reflections and to reduce Fabry–Perot resonance inside the device.

Polarization-dependent coupling loss at the input/output facets was removed from the resultant measurements by normalizing the data for each polarization scan to that for an identical scan of a straight waveguide. The straight wave-

guide had the same dimensions as the waveguides used in the racetrack resonator. Figure 3(a) shows that at 1576.241, 1576.433, and 1576.624 nm the resonant minima in both the TE and TM spectral scans align to within 1 pm. Hence the device is polarization independent for these wavelengths. The dip at 1576.815 nm had a deviation between the TE and TM minima of 2 pm. The FSR was measured to be 191 and 193 pm for TE and TM polarizations, respectively. The extinction ratio was measured to be approximately 12.1 dB for TE and 11.7 dB for TM at 1576.624 nm. A close-up of the resonance dip at 1576.624 nm is shown in Fig. 3(b) and was used to measure the finesse (F) of the resonator. The finesse was calculated to be 11.9 for TM and 12.1 for TE. This means that the characteristics are almost identical for TE and TM polarizations. Over a range of four times the FSR, the dips align to within 2 pm. This very slight misalignment is due to the small difference in the propagation constants of the TE and TM modes. For switching and modulation applications that may typically be single wavelength based applications, this amounts to polarization independence to a very high specification.

We have fabricated and measured racetrack resonator on SOI that is polarization independent to within 2 pm over a spectral range of four times the FSR. This represents a significant improvement in the state of the art. The FSR was measured to be approximately 192 pm with a finesse of 12 and a Q factor of 90 000. This demonstrates that a single

mode polarization independent laterally coupled racetrack resonator is feasible in SOI, using rib waveguides. Furthermore, this approach could be used on smaller devices that require a larger FSR.

The authors would like to thank Andrew Alduino and Jeffery S. Tseng of the Intel Corporation for their contributions in sample preparation and Oded Cohen and Dani Hak of the Intel Corporation for their contributions in the fabrication of the devices.

¹B. E. Little, S. T. Chu, H. A. Haus, J. Foresi, and J.-P. Laine, *J. Lightwave Technol.* **15**, 998 (1997).

²D. G. Rabus, M. Hamacher, U. Troppenz, and H. Heidrich, *IEEE J. Sel. Top. Quantum Electron.* **8**, 1405 (2002).

³V. Van, T. A. Ibrahim, K. Ritter, P. P. Absil, F. G. Johnson, R. Grover, J. Goldhar, and P.-T. Ho, *IEEE Photonics Technol. Lett.* **14**, 74 (2002).

⁴T. A. Ibrahim, W. Cao, Y. Kirn, J. Li, J. Goldhar, P.-T. Ho, and C. H. Lee, *IEEE Photonics Technol. Lett.* **15**, 36 (2003).

⁵S. Suzuki, Y. Hatakeyama, Y. Kokubun, and S. T. Chu, *J. Lightwave Technol.* **20**, 745 (2002).

⁶P. Dumon, W. Bogaerts, J. Van Campenhout, V. Wiaux, J. Wouters, S. Beckx, and B. Roel, presented at the Lasers and Electro-Optics Society Annual Meeting, 2003 (unpublished).

⁷K. Wada, presented at the Photonics West, San Jose, CA, 2004 (unpublished).

⁸Rsoft Design Group, Inc., 200 Executive Group Blvd. Ossining, NY 10562, www.rsoftinc.com.

⁹Ibis Technology Corp., 32A Cherry Hill Drive, Danvers, MA 01923, www.ibis.com.